

Supplementary Material for:

Size-dependent patterned recognition and extraction of metal ions by a macrocyclic aromatic pyridone pentamer†

Jie Shen,^a Wenliang Ma,^b Lin Yu,^b Jin-Bo Li,^c Hu-Chun Tao,^c Kun Zhang,^b and Huaqiang Zeng^{*a}

^a Institute of Bioengineering and Nanotechnology, 31 Biopolis Way, The Nanos, Singapore 138669. E-mail: hqzeng@ibn.a-star.edu.sg; Tel: +65-6824-7115

^b Faculty of Chemical Engineering and Light Industry, Guang Dong University of Technology, Guang Dong, China 510006. China

^c Key Laboratory for Urban Habitat Environmental Science and Technology, School of Environment and Energy, Peking University Shenzhen Graduate School, Shenzhen 518055, China

Corresponding Author: hqzeng@ibn.a-star.edu.sg

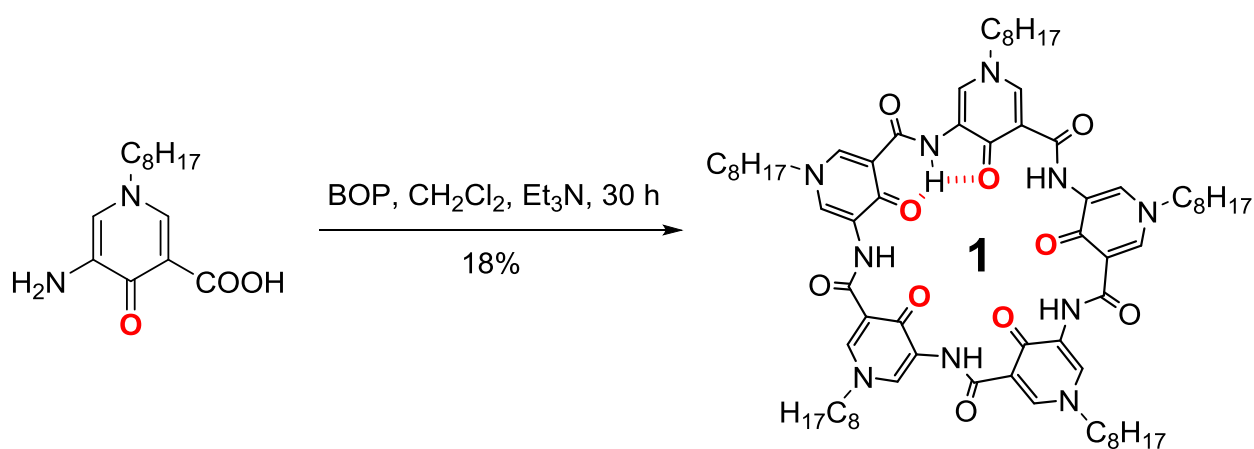
1. General Remarks and Synthesis of Pentamer 1.....	S2
2. Association Constants K_a (Table S1).....	S3
3. Inductively Coupled Plasma Mass Spectrometry (ICP-MS).....	S3
4. General Description of First Principle Computation and Optimized Structures....	S4
5. Rationale on the Use of Computationally Determined $1 \bullet M^{n+}$ Complexes Containing no Water Molecules to Explain the Observed Size-dependent Extractions by 1.....	S7

1. General Remarks

All the reagents were obtained from commercial suppliers and used as received unless otherwise noted. Aqueous solutions were prepared from distilled water. The organic solutions from all liquid extractions were dried over anhydrous Na_2SO_4 for a minimum of 15 minutes before filtration. Reactions were monitored by thin-layer chromatography (TLC) on silica gel pre-coated glass plates (0.25 mm thickness, 60F-254, E. Merck). Flash column chromatography was performed using pre-coated 0.2 mm silica plates from Selecto Scientific. Chemical yield refers to pure isolated substances. The pentamer product **1** was confirmed by its ^1H NMR, ^{13}C NMR and mass data.

For synthesis of the following pentamer **1**, see: Z. Y. Du, C. L. Ren, R. J. Ye, J. Shen, Y. J. Lu, J.

Wang and H. Q. Zeng, *Chem. Commun.* 2011, **47**, 12488.



2. Association Constants K_a (Table S1)

Table S1 Association constants $K_a^{a,b}$ for **1** complexing alkali picrate salts from Li^+ to Cs^+ in $\text{H}_2\text{O}/\text{CHCl}_3$ at 25 °C determined by Cram's method.⁷

	Li^+	Na^+	K^+	Rb^+	Cs^+
K_a ($\times 10^{-8}$ M)	2.28	1.78	0.57	0.24	0.18

^a [Guest] and [Host] at 10 mM. ^b Averaged values over three runs with standard deviations of ≤ 0.10 and with the assumption of 1:1 guest:host binding stoichiometry.^{2b}

3. Inductively Coupled Plasma Mass Spectrometry (ICP-MS)

All the chemicals were obtained from commercial suppliers and used as received unless otherwise noted. Aqueous solutions were prepared from MiliQ water. The ICP data were recorded on Thermo Fisher X Series 2. And Hg^{2+} detection however was carried out by using Analytik Jena mercur plus Hg.

For ICP measurements, The concentration of each metal ion is set at 0.10 mM with a total concentration of 1.80 mM involving all 18 ions in H_2O containing 1% HNO_3 , and that of macrocyclic hosts **1** and 18-crown-6 ranges from 0.12 mM to 1.80 mM in CHCl_3 while the concentration of 21-crown-7 and valinomycin is 3.60 mM. Extractions were carried out in a biphasic system using equal volumes of H_2O containing metal ions and CHCl_3 containing organic host at 25 °C. The [host]/[individual metal ion] ratio ranges from 1.2, 5.4, 9.0 to 18 for **1** and 18-crown-6. All the reported data are averaged values over six runs with relative errors within 3%, and only extraction efficiencies of $\geq 6\%$ are listed..

4. General Description of First Principle Computation and Optimized Structures

All the calculations were carried out by utilizing the Gaussian 09 program package.¹ The geometry optimizations were performed at the density functional theory (DFT) level, and the Becke's three parameter hybrid functional with the Lee-Yang-Parr correlation functional (B3LYP)² method was employed to do the calculations. The 6-31G(d,p)³ basic from the Gaussian basis set library has been used in all the calculations in Chloroform. The harmonic vibrational frequencies and zero-point energy corrections were calculated at the same level of theory.

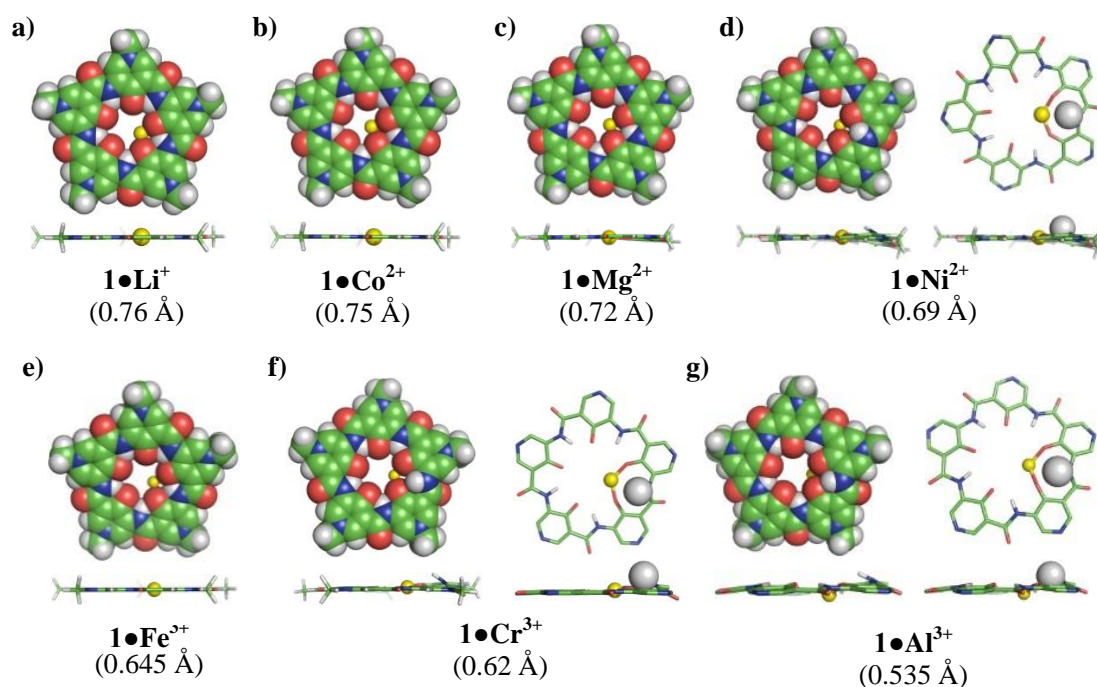


Fig. S1 Computationally optimized structures of $1\bullet\text{M}^{\text{n}+}$ at the level of B3LYP/6-31G(d,p) in chloroform. All the CPK models were built based on the van der Waals radius (Gray: H = 1.20 Å; Green: C = 1.70 Å; Blue: N = 1.55 Å; Red: O = 1.52 Å). The yellow atoms in all the structures refer to metal cations whose radii were specified in the respective parenthesis. With ions being forced into the vicinity of one of the five partially positively charged amide H-atoms in d)-f), the amide H-atom is forced to point away from the molecular plane due to the strong repulsions between ions and H-atoms.

¹ Frisch, M. J.; et al. *Gaussian 09*; Gaussian, Inc.: Wallingford CT, 2009.

² Becke, A. D. *J. Chem. Phys.* **1993**, 98, 5648.

³ Petersson, G. A.; Al-Laham, M. A. *J. Chem. Phys.* **1991**, 94, 6081; Petersson, G. A.; Bennett, A.; Tensfeldt, T. G.; Al-Laham, M. A.; Shirley, W. A.; Mantzaris, J. *J. Chem. Phys.* **1988**, 89, 2193.

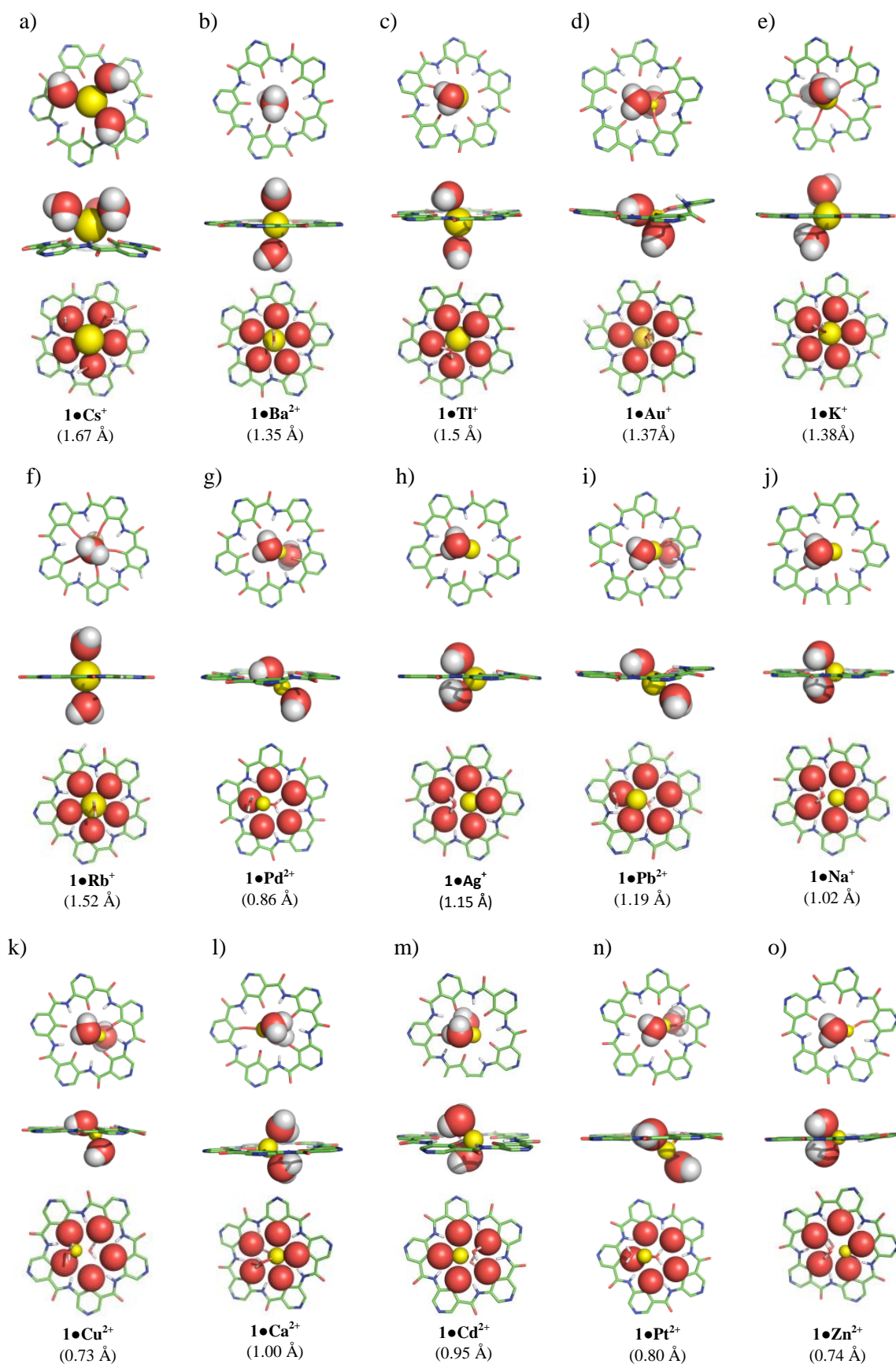


Fig. S2 Computationally optimized structures of water-containing complexes **1•M^{II+}** at the level of B3LYP/6-31G(d,p) in chloroform. All the CPK models were built based on the van der Waals radius (Gray: H = 1.20 Å; Red: O = 1.52 Å). The yellow atoms in all the structures refer to metal cations whose radii were specified in the respective parenthesis.

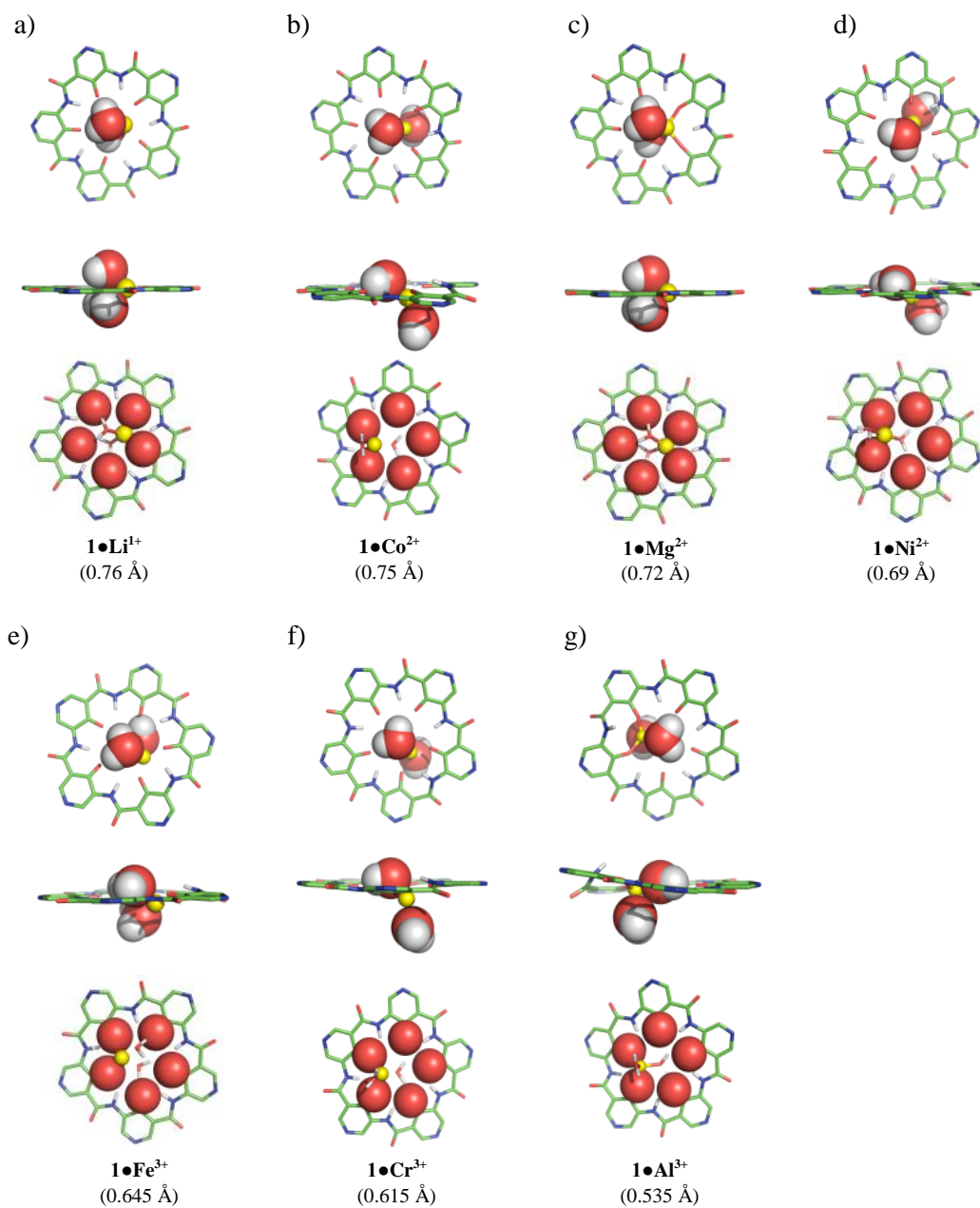


Fig. S3 Computationally optimized structures of water-containing complexes **1•Mⁿ⁺** at the level of B3LYP/6-31G(d,p) in chloroform. All the CPK models were built based on the van der Waals radius (Gray: H = 1.20 Å; Red: O = 1.52 Å). The yellow atoms in all the structures refer to metal cations whose radii were specified in the respective parenthesis.

5. Rationale on the Use of Computationally Determined $1 \bullet M^{n+}$ Complexes Containing no Water Molecules to Explain the Observed Size-dependent Extractions by **1**

The binding of metal ions by pentameric host **1** apparently involves two steps. In step 1, the fully naked ions are brought into the planar cavity of **1**. Upon binding by planar **1**, these metal ions need only two more water molecules to satisfy their six-coordinate requirement, which can be easily accomplished in step 2 where the two water molecules approach the pentamer-metal ion complex from the two unoccupied axial positions. Regardless of whether steps 1 and 2 proceed in sequential or concurrent fashions and how complicated the binding process could be, the ability of the metal ions to fit inside the cavity as well as possible, to form as many coordination bonds as possible and to produce the minimum distortion of the pentameric backbone of **1** in step 1 is a real factor and should constitute one of decisive factors that helps to determine the binding of ions by **1** (other primary factors may include the energetic loss in “stripping off” four water molecules occupying the same plane by **1** in step 1, energetic gain from the formation of coordination bonds between **1** and metal ions, and hydration energy involving two axially coordinated water molecules in step 2. Certainly, the situation will become more complicated if the interactions of host molecule with water and (de)hydration energy involving secondary hydration shell are further considered). Since the two axially coordinated water molecules always stay associated with the metal ions before or after the binding of metal ions by **1**, the computationally determined pentamer-metal ion complexes without two axially coordinated water molecules should allow us to qualitatively explain the observed trend. If metal ions do not fit into the cavity well, then the resulting energetic penalties arising from distorting the pentameric backbone of the host plus dehydration energy involving four water molecules must be paid for by coordination bonds formed between pentamer and metal ions. In the simplest scenarios where the coordination energy provided by pentamer is equal to or less than the dehydration energy involving removing four water molecules from metal ions upon the formation of pentamer-metal ion complexes, then the distortion of the pentameric backbone in **1** caused by the binding of metal ions will have to be fully compensated for by the hydration energy involving two axially coordinated water molecules. However, this compensation is unlikely to happen in many cases (or could be insufficient) since the two axially coordinated water molecule already stay associated with the metal ions before binding of metal ions by **1**. These scenarios probably are applicable to metal ions with very small radii that lead to the formation of two

coordination bonds between host and metal ions, which is not sufficiently large enough to remove four water molecules associated with the metal ions to form the complex. Therefore, even though the structures for pentamer-metal ion complexes with and without axially coordinated water molecules could be different, the optimized structures without axially coordinated water molecules should provide good insights for us to qualitatively explain the observed trend on the “size-dependent” extractions by **1**.

Nitrate anions generally stay outside the first hydration shell and should not be the decisive factor that determines the ion binding by **1**. For examples on the nitrate salts of Mg^{2+} , Fe^{3+} and Al^{3+} where nitrate anions bind metal ions less strongly than water molecules, and so stay outside the first hydration shell that is octahedral, see *Mater. Res. Bulletin*, **1995**, *30*, 1235, *Inorg. Chem.*, **1977**, *16*, 245 and *Acta Cryst.*, **1983**, *C39*, 925, respectively. Even if in some cases, the nitration anions bind to **1** more strongly than water molecules, they probably won't affect the binding of metal ions by **1** to appreciable extents since **1** bearing a planar backbone has two axial vacancies that are available for counter anions. That means, tightly associated nitrate anions can always stay tightly associated with metal ions for mono- and divalent metal ions before and after extractions, and so probably should not dramatically interfere with the binding of metal ions by the host.

By assuming a seven-coordinate environment for Cs^+ for which three water molecules are coordinated to Cs^+ from the same side in $\mathbf{1}\bullet\text{Cs}^+$ complex and a six-coordinate environment for all the other metal ions for which two water molecules are axially coordinated to M^{n+} from different sides in $\mathbf{1}\bullet\text{M}^{n+}$ complexes, we have computationally optimized $\mathbf{1}\bullet\text{Cs}^+$ complex containing three water molecules on the same side, and another twenty-one $\mathbf{1}\bullet\text{M}^{n+}$ complexes containing two water molecules occupying two axial positions. For unknown reasons, complex $\mathbf{1}\bullet\text{Mn}^{2+}$ containing water molecules cannot be computationally optimized. It is interesting to note that all the highly distorted structures without water molecules (Figure 1k-m and 1p) now become planar upon the addition of two water molecules at axial positions (Figures S2-3). This suggests that energy for re-planarizing the distorted backbones in host **1** caused by metal ions be paid for by hydration or coordination energies. As discussed above, our use of the structures without water molecules to qualitatively explain the observed size-dependant extractions should still hold true. These computationally determined structures with water molecules have been added into SI as Figures S2-3.